

# MICROWAVE CHARACTERIZATION OF THIN FERROELECTRIC FILMS

A. Deleniv\*, S. Abadei\*, and S. Gevorgian\*<sup>#</sup>

\* Department of Microtechnology and Nanoscience MC-2, Chalmers University of Technology  
41296 Gothenburg, Sweden: [anatoli@ep.chalmers.se](mailto:anatoli@ep.chalmers.se), [abadei@ep.chalmers.se](mailto:abadei@ep.chalmers.se),  
[spartak@ep.chalmers.se](mailto:spartak@ep.chalmers.se)

<sup>#</sup> Microwave and High Speed Research Center, Ericsson Microwave Systems  
431 84 Moelndal, Sweden

**Abstract** — A simple technique for characterization of dielectrics at high microwave frequencies is presented and demonstrated. The technique makes use of the measured impedance of a test structure. The latter is a simple capacitor, formed on the top of a substrate with an arbitrary number of dielectric/conductor layers and contains a material under test (MUT) layer with unknown loss tangent and dielectric constant. Assuming that all other layers are specified, a simple method is given to calculate RF impedance of such a structure enabling extraction of MUT properties.

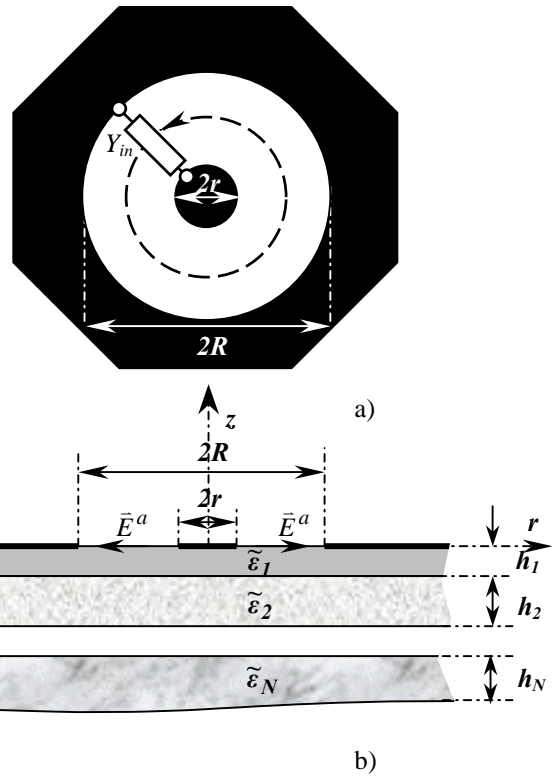


Fig. 1 Layout (a) and cross-section (b) of the test-structure.

## I. INTRODUCTION

In this paper we propose a test structure for microwave characterization of dielectric layers in a multiplayer dielectric stack, based on microprobe measurements. The test structure used for measurements is shown in Fig.1. It is similar to the one proposed in [1], but in general it does not require a ground electrode between layers 1 and 2. One port reflection measurement of the complex impedance is considered here. A simple model for the impedance of the test structure is developed that enables accurate computation of dielectric properties of material under test (MUT). Cylindrical symmetry of the structure, Fig.1, makes the analyses quite simple and accurate. The model is based on the reaction concept applied in the Hankel transform domain.

## II. TEST STRUCTURE

Each substrate layer (except MUT) is characterized by complex permittivity  $\tilde{\epsilon}_i$  and thickness  $h_i$ . From beneath/above the structure is terminated by an arbitrary impedance condition (electric/magnetic wall or infinitely extended media). A capacitor is formed on the top of the substrate with characteristic dimensions  $2r$  and  $2R$  as it is shown in Fig.1. In the following we assume that quality factor of such a capacitor is mainly defined by the layered substrate (electrodes are lossless).

## II. TEST STRUCTURE MODELING

We start with a stationary formula for admittance [2]:

$$Y_{in} = \frac{\langle a, a \rangle}{V^2} = \frac{-\iint H^a \cdot M^a ds}{V^2} \quad (1)$$

where  $\langle a, a \rangle$  is a self-reaction or a reaction of the field on its own voltage source  $V$  (integration is taken over the over location of magnetic current). The latter is defined as two sheets of inversely directed impressed magnetic current  $M^a$ , which are placed beneath and above the perfectly conducting ring interface in a way to complement the metal free area

of the test structure aperture. The upper surface of such a voltage source is shown schematically in Fig.2. Being inserted into aperture such a voltage source produces a positively directed terminal field  $E_r^a = -M_\phi^a$  as it is shown in Fig.1b.

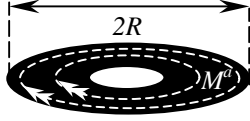


Fig.2 Equivalent voltage source representation using inversely directed sheets with magnetic current.

Then the expression (1) can be rewritten in rather accommodative for our purpose form:

$$Y_{in} = \frac{\langle a, a \rangle}{V^2} = \frac{\iint J^a \cdot E^a ds}{V^2} \quad (2)$$

where  $J^a$  is an induced current through the voltage source and integration is only over the aperture - the only area with non zero electric field. In the next step we define the field-current connection in the Hankel transform domain (HTD). Considering no angular dependence of the electric field (we restrict our self by frequencies well below the first resonance) we obviously deal with  $TM$ -to- $z$  field. Thus, the following equality holds in the HTD [3] (hereafter subscript  $r$  will be skipped, since these are only components considered herein):

$$\tilde{J}(k\rho) = Y\tilde{e}(\omega, k\rho) \tilde{E}(k\rho) \quad (3)$$

where  $Y\tilde{e}(\omega, k\rho)$  is a  $TM$ -to- $z$  wave admittance seen from the interface with impressed electric field:

$$\tilde{E}(k\rho) = \int_r^R E(r) J_1(k\rho r) r dr \quad (4)$$

In the next step the trial field has to be defined. We assume that latter is a linear combination of following basis functions:

$$E_n^a(x) = \frac{T_n\left(\frac{x-0.5(R+r)}{0.5(R-r)}\right)}{x^2 \sqrt{1 - \left(\frac{x-0.5(R+r)}{0.5(R-r)}\right)^2}} \quad (5)$$

where  $T_n$  is  $n$ -th order Chebyshev polynomial and  $R(r)$  is the outer (inner) radius of the aperture. Such a choice of trial functions is quite beneficial, since a closed form expression can be derived for large argument of  $\tilde{E}_r(k\rho)$ , leading to rather efficient computational routine.

Omitting some tedious intermediate derivation and noting that  $\iint J^a \cdot E_n^a ds = I_{in} V_n$  for any  $n$ , where  $I_{in}$  is the input current and  $V_n$  is the voltage of  $n$ -th trial field basis function at the input, we arriving to the following equality for self reaction:

$$\langle a, a \rangle = I_{in} \begin{bmatrix} V_1 \\ \vdots \\ V_n \end{bmatrix}^T \begin{bmatrix} \langle J_1^r, E_1^r \rangle & \cdots & \langle J_1^r, E_n^r \rangle \\ \vdots & \ddots & \vdots \\ \langle J_n^r, E_1^r \rangle & \cdots & \langle J_n^r, E_n^r \rangle \end{bmatrix}^{-1} \begin{bmatrix} V_1 \\ \vdots \\ V_n \end{bmatrix} I_{in}$$

or

$$\langle a, a \rangle = I_{in}^2 [V]^T [Matr]^{-1} [V] \quad (6)$$

where reactions are defined in the HTD as:

$$\langle J_i^r, E_j^r \rangle = 2\pi \int_0^\infty \tilde{Y}e(\omega, k\rho) \tilde{E}_i^r(k\rho) \tilde{E}_j^r(k\rho) k\rho dk\rho \quad (7)$$

Inserting (6) into (2) we obtained the final expression for input admittance used in our codes:

$$Y_{in} = \left( [V]^T [Matr]^{-1} [V] \right)^{-1} \quad (8)$$

At this point it seems important to note that the test structure admittance as it is given by (8) is related to the test structure aperture (metal free area) with circularly shaped terminals defined precisely by aperture boundaries, as it is shown in Fig.1a. It is clear that measured impedance of the test structure using coplanar microprobes will include a parasitic inductance due to the finite current path between probe tips and aperture terminals, thus it is important to take this parasitic inductance into account. To remove this parasitic inductance we have made a modification in the calibration routine discussed in the next section.

### III. VERIFICATION OF THE MODEL

First we checked the convergence of (8). We assume test structures with apertures  $R-r=2.5\mu m$  and  $70\mu m$  and  $R=100\mu m$  fixed outer radius. The computed results for structures consisting of  $400\mu m$  thick silicon substrate ( $\epsilon_r=11.7$ ) on top of  $5mm$  thick teflon holder ( $\epsilon_r=2.1$ ) are presented in Table1 for  $f=10GHz$ . As it follows from the Table the only one

Table1. Capacitance convergence at 10GHz

$C(pF)$	Number of trial functions			
	1	2	3	4
$C(2.5 \mu m)$	.11416	.11414	.11414	.11414
$C(70 \mu m)$	.01853	.01551	.01542	.01542

term in the trial field expansion is enough to obtain accurate result for  $2.5\mu m$  case, while for wider apertures the number of trial functions has to be increased. This claim should be considered only as general trend, since for very thin layers even for narrow apertures more trial functions may be needed.

To verify the proposed model experimentally, we fabricated a number of structures with fixed outer radius  $R=100\mu m$ , using inner radius as a parameter. MgO and Si substrates are used in the experiments.

The test structure on MgO substrate is used for measurements of the losses in copper electrodes.

Microwave measurements are performed using VNA and SOL (Short-Open-Load) calibration (GSG-200 microprobes from Picoprobe GGB). It is recommended by manufacturer (Picoprobe GGB) that probe tips be placed at certain distance from the edges of the test structure to ensure a reliable contact. Then the part of the test structure between probe tips and the edge of the test structure appears as a negative capacitance where the probe is lifted above the substrate. However, in our case it causes a systematic measurements error, since we do not have open-end edges in our test structure, Fig.1a. Hence, the negative capacitance discussed above should not be taken into account in our measurements.

As we already mentioned in the previous section, the measured admittance includes not only the aperture admittance, but also parasitic inductances between the probe tips and the edges of aperture as shown in Fig.3. The effect of the parasitic inductance will be significant if its reactance is compatible with reactance of the test structure. Thus, this parasitic inductance should be removed to avoid frequency dependence (dispersion), which has nothing to do with the capacitance of the test structure.

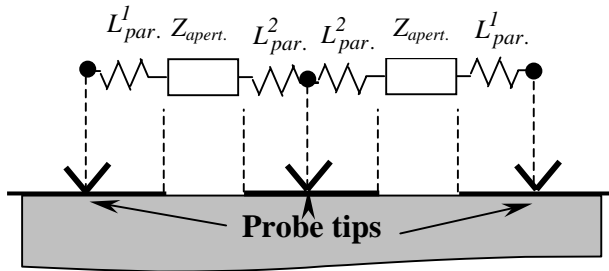


Fig.3 Schematic representation of the circuit seen by VNA.

Two different curves are presented in Fig.4 obtained using standard and modified calibration procedures, demonstrating the importance in distinguishing these effects. Two modifications as compared to standard were used in our calibration: the open standard (0F) is assigned to the lifted above the metallized plane probe, while short standard (0H) is realized as simple contact of probe with metallized plane (in this way we remove all parasitic inductance effects).

Two sets of simulated in accordance to the model curves for test structure capacitances on MgO and Si substrates are compared with measured values in Fig.5, thereby validating accuracy of both, model and calibration. The quality factor of test structure on MgO substrate is typically too high to be measured accurately (using present technique), which supports the above claim regarding small electrode losses. It also shows that measured quality factor for test structure on Si may be attributed only to finite

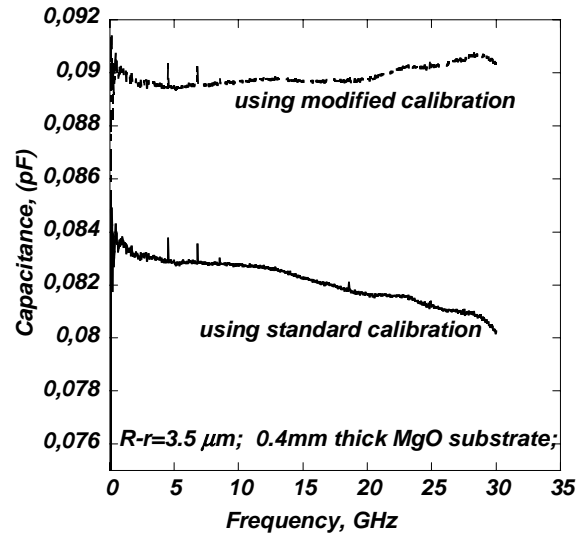


Fig.4 Measured test structure capacitance using standard and modified calibration.

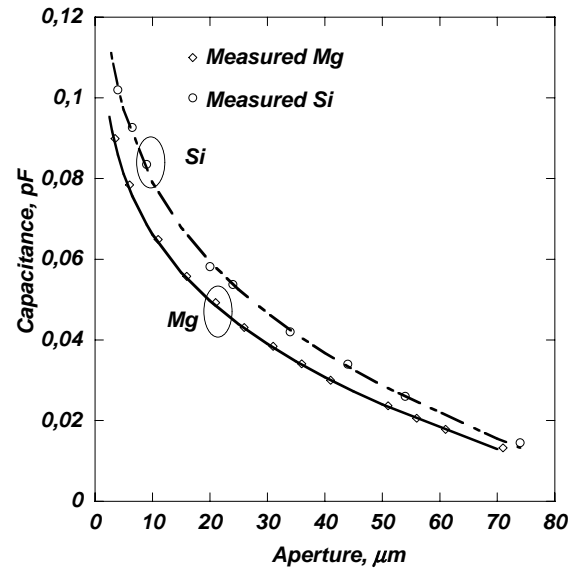


Fig.5 Comparison of simulated and measured test structure capacitances.

resistivity  $\rho$  of the substrate. Measured ( $\tan \delta_{eff.} = 1/Q$ ) and theoretical values of loss tangent ( $\tan \delta_{eff.} = 1/\omega \epsilon_0 \epsilon_r \rho$ , [4] above Maxwell relaxation frequency) for  $\rho=1k\Omega \cdot cm$  silicon substrate are plotted in Fig.6.

## V. APPLICATION EXAMPLE

Often there is a need to characterize rather lossy MUT with typical  $\tan \delta \approx 0.02 \div 0.05$  (e.g. ferroelectrics films). The cross-section of a test structure with ferroelectric film and measured capacitance are given in Fig.7. As before we kept fixed outer radius  $R=100\mu m$ , while the aperture has three different options ( $R-r=5; 7.5; 22.5\mu m$ ). Simulated capacitances

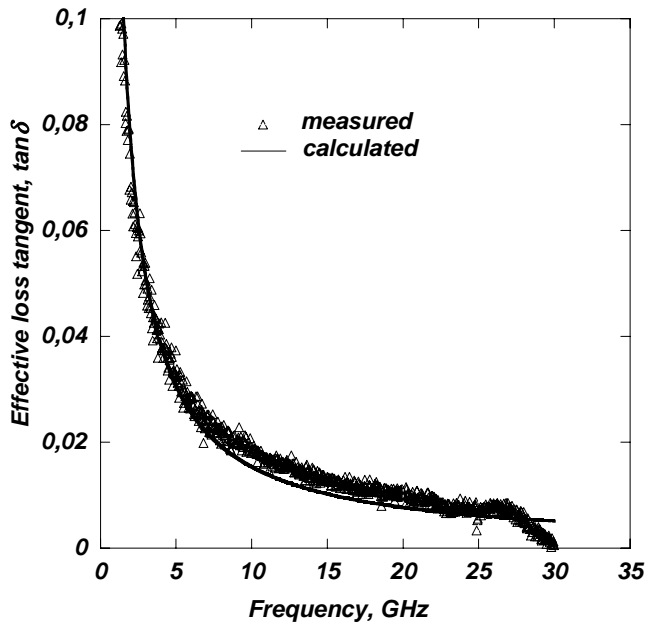


Fig.6 Measured and theoretical loss tangent of  $\rho=1\text{k}\Omega\cdot\text{cm}$  silicon.

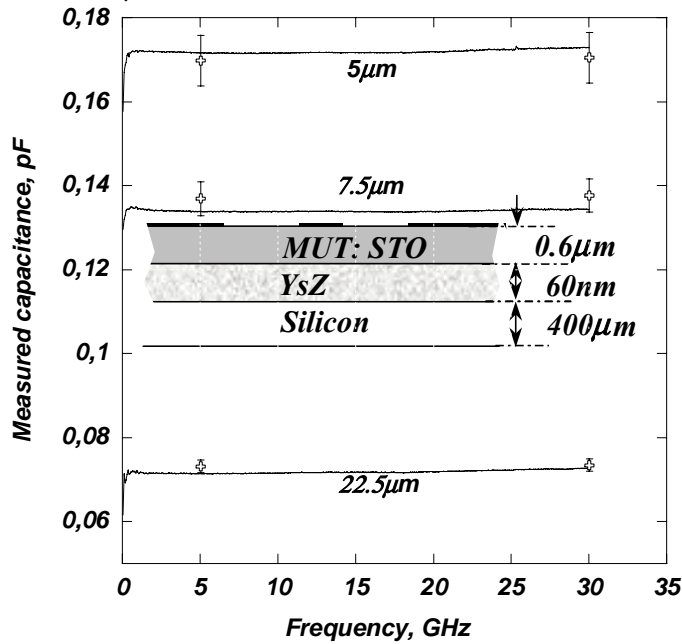


Fig.7 Measured capacitance for the structure with cross-sectional view.

for these geometries are also presented in this plot (marked by small crosses) with bars delimiting  $\epsilon_r=125\pm 10$  range of used in simulation dielectric constant at two fixed frequency points  $f=5;30$  GHz. Measured frequency dependent effective loss tangent of the test structure with  $5\mu\text{m}$  aperture is shown in Fig.8. Two different regions with losses associated with the silicon substrate (below 5GHz) and STO film (above 5GHz) can be clearly distinguished. Using the model it is also possible to extract the losses in STO film. It was found that  $\tan \delta_{STO} = 0.03$  at 10GHz and  $\tan \delta_{STO} = 0.057$  at 30GHz respectively.

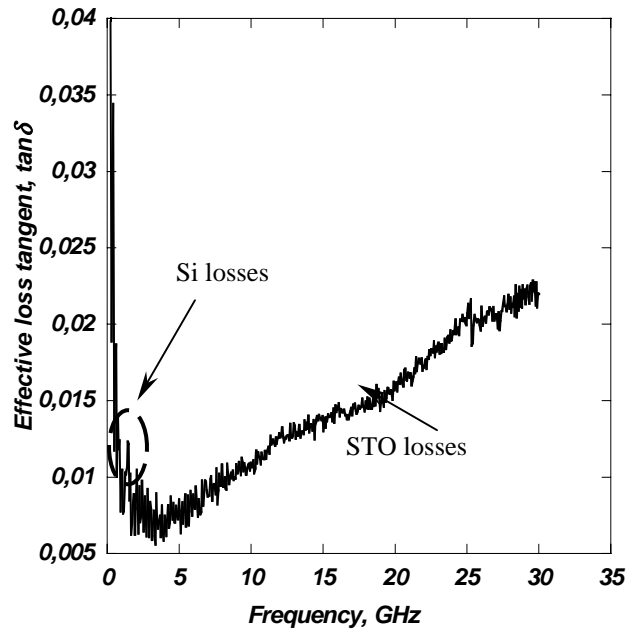


Fig.8 Measured effective loss tangent of the test-structure containing STO layer.

#### ACKNOWLEDGEMENT

The authors wish to acknowledge support of Vetenskapsrådet (Swedish Science Foundation) and CHACH (Chalmers Center for High Speed Technology).

#### REFERENCES

- [1] Z. Ma, Andrew J. Becker, P.Polakos, H. Huggins, J. Pastalan, Hui Wu, K.Watts, Y.H.Wong, and P. Mankiewich, "RF Measurement" Technique for Characterizing Thin Films", IEEE Trans. Electron. Devices.
- [2] Roger F. Harrington, "Time-Harmonic Electromagnetic Fields", McGraw-Hill, Inc., 1961.
- [3] Kiyomichi Araki and Tatsuo Itoh, "Hankel Transform Domain Analysis of Open Circular Microstrip Radiating Structures", IEEE Trans. Antenna and Prop., Vol.AP-29,pp.84-89.
- [4] S. Gevorgian, "Surface Impedance of Silicon Substrates and Films", Int. J. RF and Microwave CAE, 1998, pp.433-439.